# Describing Asymmetric Hysteretic $F-V$ Characteristics of a MR Damper Resulted from Symmetric MR Damper

Wang Enrong[1], Wang Wanjun[1], Wang Hui[1], Rakheja Subhash[2], Su Chunyi[2]

(1. School of Electrical and Automation Engineering, Nanjing Normal University, Nanjing 210042, China;
2. Department of Mechanical and Industrial Engineering, Concordia University, H3G 1M8, Montreal, Canada)

**Abstract**: To achieve intelligent vehicle suspension with magneto-rheological (MR) fluids dampers, extensive laboratory measurements are performed to test the hysteretic force-velocity ($f-v$) characteristics of a MR-damper, under a wide range of drive current and harmonic excitation conditions (frequency and stroke). The proposed asymmetric damping force generation (ADFG) algorithm is employed to generate the asymmetric damping force in compression and rebound from a symmetric MR-damper design, and the proposed generalized model is employed to characterize both symmetric and asymmetric hysteretic $f-v$ characteristics. The measured data are used to identify the model parameters, and the model results are compared with the measured data to assess effectiveness of the proposed model synthesis. The results show reasonably good agreements between model results and measured data, irrespective of excitation conditions and drive current, and thus verify that the proposed ADFG algorithm can be used as a fundamental control policy for yielding asymmetric $f-v$ characteristics from the symmetric MR-damper design.

**Key words**: magneto-rheological fluids damper; asymmetric damping; hardware-in-the-loop test; model
**CLC number**: TH 703. 62, **Document code**: B, **Article ID**: 1672-1292(2008)01-0001-06

# 由对称型 MR 阻尼器产生不对称滞环 $F-V$ 特性的描述

王恩荣[1], 王皖君[1], 王 惠[1], Rakheja Subhash[2], Su Chunyi[2]

(1. 南京师范大学电气与自动化工程学院, 江苏 南京 210042; 2. 康考迪亚大学机械与工业工程系, 加拿大 H3G 1M8)

[摘要] 为实现磁流变阻尼器驱动的智能车辆悬架设计, 在大范围驱动电流和谐波激励条件(频率和幅度)下, 对一 MR 阻尼器进行了大量的阻尼力-速度($f-v$)特性测试实验研究. 应用提出的不对称阻尼力产生(ADFG)算法, 由该对称型阻尼器产生不对称的延伸和压缩阻尼力, 并应用提出的通用模型来描述对称和不对称滞环 $f-v$ 特性. 测试数据用来对模型参数进行辨识, 并将模型计算结果与测试数据进行比较来验证所提模型的正确性. 表明模型计算结果与测试数据在任意的激励条件和控制电流下均具有很好的一致性, 因此证明所提出的 ADFG 算法可作为一基本的控制算法来实现从对称型 MR 阻尼器设计产生不对称 $f-v$ 特性.

[关键词] 磁流变阻尼器, 不对称阻尼, 硬件在环测试, 模型

The magneto-rheological (MR) fluid-based damper have been widely explored for their potential implementation in vehicle suspension and shown its superior potential performance benefits in relation to conventional hydraulic dampers[1-4]. The requirement of adequate ride, road-holding, handling and directional control stability performance of road vehicles entails variable damping, which could be achieved with MR dampers with only minimal power consumption, unlike a fully active suspension which could add or remove energy depending upon the demand with the help of an elaborate power supply. The semi-actively controlled MR-fluid dampers exhibits highly nonlinear variations in damping force, attributed to the hysteresis and force-limiting properties of the fluid as functions of intensity of applied magnetic field, and displacement and velocity of the piston, and offer rapid vari-

**Received date**: 2008-01-12.
**Foundation item**: Supported by Provincial Six Categories of Summit Talents of Jiangsu (No. 2006194) and Scientific Research Foundation of Education Ministry of China ([2007] No. 1108).
**Biography**: Wang Enrong (1962-), professor, field of study: semi-active control for implementing intelligent vehicle suspension with MR-fluid dampers and electrical engineering, etc. E-mail: enwang@njnu.edu.cn

ations in damping properties in a reliable fail-safe manner, since they continue to provide adequate damping in a passive manner in the event of control hardware malfunction[4]. However, the reported MR-fluid dampers have been mostly developed to yield symmetric damping forces in compression and rebound when the excitation is of symmetry. The vehicle suspension designs generally require the asymmetric dampers for improving the road holding and ride suspension requirements[5, 6], it is thus essential to synthesize a fundamental controller algorithm to yield the asymmetric force-velocity ($f-v$) characteristics from the symmetric MR-damper design.

In this study, the proposed asymmetric damping force generation (ADFG) algorithm[6] is employed to modulate the drive current in asymmetric mode to generate the asymmetric damping force in compression and rebound for a symmetric MR-damper design, and extensive laboratory tests are performed to characterize both symmetric and asymmetric dependence of hysteretic damping force of a candidate MR-damper under a wide range of drive current and excitation conditions (frequency and stroke). The proposed generalized MR-damper model[7] is further employed to characterize the symmetric and asymmetric hysteretic $f-v$ characteristics of the controllable MR dampers. The generalized model synthesis in conjunction with the measured data of both symmetric and asymmetric damping characteristics are used to identify the model parameters. Simulations are performed to assess the effectiveness of the proposed model synthesis, and results obtained under wide range of simulation conditions are compared with those obtained from the measured data. It is noted that the study has been partly published in the recent WSEAS international conference as an invited plenary lecture[8].

## 1 Characterization of Symmetric and Asymmetric Hysteretic $F-V$ Characteristics

A MR-damper, developed by CARRERA[9] and pictorially shown in Fig 1, is considered for characterizing its damping properties in the laboratory. The considered damper, designed for automotive applications, could provide a total stroke of 200 mm. The damper is a mono-tube design and comprises floating piston, which separates the MR-fluid and gas media. The piston is designed with annular orifices, and comprises electro-magnetic coils to generate magnetic field in response to an applied electric current. The variations in viscous and shear properties of the fluid, caused by the applied magnetic field, yield variations in damping force developed by the damper, and a direct current limited to 0.5 A at 12 V serves as command signal for the coils.

**Fig.1 A pictorial view of a candidate MR-damper**

### 1.1 Test Apparatus and Methodology

A Hardware-in-the-loop (HIL) test platform, as shown in Fig 2, is developed in the laboratory for this study[5]. A voltage-to-current circuit is designed to realize different constant levels of current excitations for the coil. The candidate MR-damper is installed on an MTS electro-hydraulic vibration exciter between the exciter and a fixed inertial frame through a force transducer. Position (LVDT) and velocity (LVT) sensors are also installed on the exciter to measure instantaneous position and velocity of the damper piston. The damper is subject to harmonic displacement excitations of different constant amplitudes at selected discrete frequencies to characterize its properties over a wide range of excitations. The force, velocity and displacement data, acquired through a data acquisition board, are directly imported into an Excel

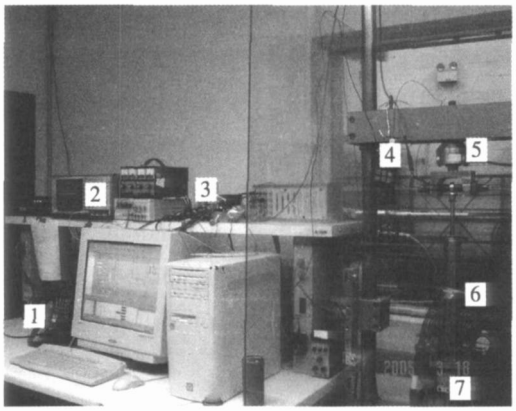


1.Servo-controller, 2.Data acquisition, 3.DC power supply, 4.Temperature monitor, 5.Force transducer; 6.MR-damper, 7.Hydraulic actuator

**Fig.2 A pictorial view of MR-damper test system**

worksheet using Dynamic Data Exchange to obtain an on-line display of the hysteretic $f-v$ characteristics. A dual regulated DC power supply is used to supply the command current to the damper. A thermocouple is also mounted on the damper body to monitor the damper temperature. The experimental data under each condition are acquired in the vicinity of a defined temperature range ($40 \pm 10$℃), so as to suppress thermal effects in the characterization task.

The measurements are initially performed under low amplitude excitation at a frequency of 0.1 Hz and the measured force is considered to represent the seal friction, assuming negligible contributions due to MR-fluid damping at extremely low velocities. The damper is then subjected to a selected excitation condition and current using the servo-controller and the voltage-current circuit, respectively, and the amplitudes of displacement excitations at higher frequencies are limited to lower values to ensure damper operation within safe velocity limits. The measured signals are displayed in the form of time-histories and Lissajuous curves in force-velocity ($f-v$) and force-displacement ($f-d$) corresponding to each test condition. The acquired data are subsequently analyzed to characterize important properties of the MR-fluid damper.

### 1.2 Symmetric Hysteretic $f-v$ Characteristics

Owing to symmetric damping design of the damper, a voltage-to-current circuit is initially applied to obtain the $f-v$ characteristics, symmetric in compression and rebound, under a fixed drive current and harmonic excitation. The symmetric hysteretic $f-v$ characteristics of the candidate damper are measured under sinusoidal displacement excitations at several discrete frequencies in the 0 to 15 Hz range, which is considered to represent the range of predominant vehicular motions along the vertical axis. The tests are performed under different constant magnitudes $a_m$ of displacement, ranging from 2.5 to 75 mm, and command current $i_d$ in the 0 to 0.4 A range. The $f-v$ characteristics measured under a few selected excitation conditions are initially analyzed to build an understanding of dynamic behaviour of the MR-damper.

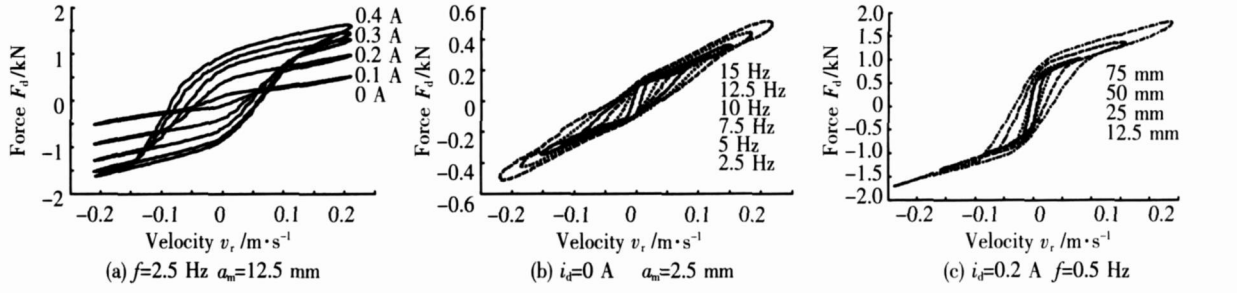


**Fig.3 Measured symmetric $f-v$ characteristics of a MR-damper under different drive current and harmonic excitation conditions**

Fig. 3 illustrates a group of symmetric hysteretic $f-v$ characteristics measured under selected harmonic excitations and drive currents. Fig. 3(a) shows the measured $f-v$ characteristics under different drive currents, at 2.5 Hz harmonic excitation with amplitude of 12.5 mm, where the damping force strongly depends on both drive current ($i_d$) and damper velocity ($v_r = \dot{x}_r$), and behaviors nearly linear rise at low velocities in the pre-yield and force saturation at higher velocities in the post-yield. Fig. 3(b) and (c) further show that the nonlinear damping properties are also strongly dependent upon the excitation frequency and amplitude, respectively. In the passive mode ($i_d = 0$), shown in Fig. 3(b), the damping force varies nearly linearly with velocity, particularly at frequencies above 5.0 Hz, and the change in the damping coefficient observed at the onset of post-yield tends to diminish under higher excitation.

The above results reveals that the damping properties of the candidate damper strongly depend on the magnitudes of drive current and the excitation frequency and amplitude, and further reveals the essential dynamic behavior of the candidate MR-damper such as the controllable property, passive behavior and hysteresis phenomenon.

### 1.3 Asymmetric Hysteretic $f-v$ Characteristics

The vehicle suspensions are usually designed to realize asymmetric damping to achieve compromise among the conflicting ride, road-holding and directional control performances, whereas the candidate MR-damper is de-

signed to provide only symmetric damping force in compression ($v_r > 0$) and rebound ($v_r < 0$). For this purpose, the authors have proposed an asymmetric damping force generation (ADFG) algorithm[6], which can be employed to yield the asymmetric $f-v$ characteristics from the symmetric MR-damper design, by limiting the drive current $i_d$ to a lower value $i_L$ during compression and switching the drive current to a higher value $i_H$ during rebound motion. Such an approach, however, would cause transient responses due to switching discontinuities around $v_r = 0$, and an algebraic filtering technique without phase delay is integrated in the algorithm to suppress the current discontinuity. The asymmetric drive current of the MR-damper $i_d$ is formulated as

$$i_d = M_p(p, \xi, v_r)\, i_c, \tag{1}$$

$$M_p(p, \xi, v_r) = \frac{1+p}{2} + \frac{2}{\pi}\left[ p\,(v_r > 0) \cup (v_r \leqslant 0) - \frac{1+p}{2} \right] \left| \tan^{-1}\left( \frac{\xi v_r}{v_m} \right) \right|. \tag{2}$$

Where $M_p$ is the multiplier of the proposed ADFG algorithm, $v_m$ is the peak relative velocity, $p$ is asymmetry factor of drive current ($0 \leqslant p \leqslant 1$) and $\xi$ is smoothing factor defining the slope of the arctan function ($\xi > 0$).

By applying the proposed ADFG algorithm to modulate the drive current shown in Eq. (1), the experiments are performed to characterize the asymmetric damping force under different test conditions and using $p = 0$ and $\xi = 2$ in $M_p$ function. This would yield $i_L = 0$ and $i_H = i_d$. Fig. 4 illustrates the measured asymmetric hysteretic $f-v$ characteristics corresponding to the selected excitation conditions and $i_d$ ranging from 0 to 0.3 A. The results show that the same candidate damper can provide asymmetric damping force in compression and rebound in continuous manner. The chosen parameters of the modulation function yield asymmetric damping force ratio ($\gamma$) in the order of 4, for low velocities.

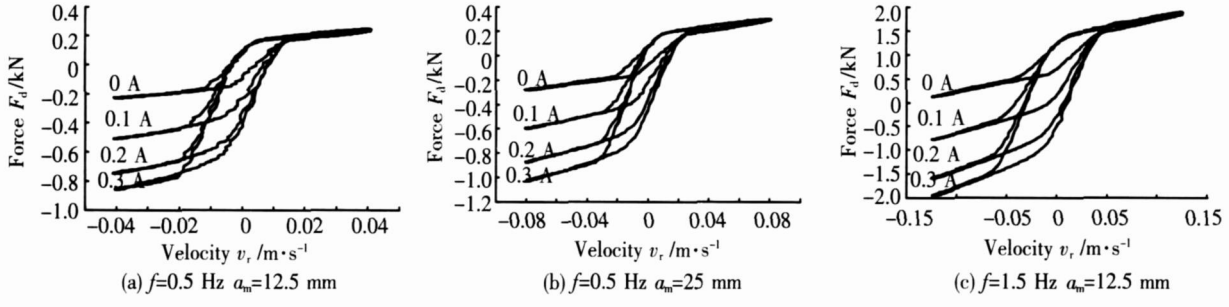


**Fig.4 Measured asymmetric $f-v$ characteristics of a MR-damper under different drive current and harmonic excitation conditions**

## 2 Modeling Symmetric and Asymmetric Hysteretic $F-V$ Characteristics

The vehicle suspension systems are generally designed with asymmetric damping characteristic to achieve a better compromise among different conflicting performance measures, while the above results show the available symmetric MR-damper can generate the acquired asymmetric damping force in rebound and compression by employing the proposed ADFG algorithm. The authors have also proposed a generalized model to characterize both symmetric and asymmetric hysteretic $f-v$ characteristics[3, 7]. The generalized hysteretic $f-v$ model is formulated as

$$F_d(v, i_d) = \begin{cases} C_i\left( F_t \dfrac{1 - e^{-\alpha(v_r + v_h + v_b)}}{1 + e^{-\alpha(v_r + v_h + v_b)}} - F_b \right) (1 + k_{vc}|v_r|) & v_r \geqslant 0, \\ C_i\left( F_t \dfrac{1 - e^{-\alpha(v_r + v_h + v_b)}}{1 + e^{-\alpha(v_r + v_h + v_b)}} - F_b \right) (1 + k_{ve}|v_r|) & v_r < 0. \end{cases} \tag{3}$$

The model involves feature parameters ($F_t$, $F_b$, $v_h$, $v_b$, $\alpha$, $k_{vc}$, $k_{ve}$) that are dependent not only on the nature of excitation $v_m$, but also on the drive current $i_d$. The transition force $F_t$, current dependent function $C_i$, constant $\alpha$, zero-force velocity intercept $v_h$, force offset $F_b$, velocity offset $v_b$, and high velocity linear rise coefficients $k_{ve}$ and $k_{vc}$ are expressed as

$$F_t = F_0\,(1 + e^{a_1 v_m}), \tag{4}$$

$$C_i(i_d) = 1 + \frac{k_2}{1 + e^{-a_2(i_d + I_0)}} - \frac{k_2}{1 + e^{-a_2 I_0}} \quad C_i(i_d) \geqslant 1, \tag{5}$$

$$\alpha = a_0 /(1 + k_0 v_m), \tag{6}$$

$$v_h = \operatorname{sgn}(\dot{x}_r) k_4 v_m \left( 1 + \frac{k_3}{1 + e^{-a_3(i_d + I_1)}} - \frac{k_3}{1 + e^{-a_3 I_1}} \right), \tag{7}$$

$$F_b = k_5 C_1 F, \qquad v_b = k_6 v_m, \tag{8}$$

$$k_{ve} = k_{1e} e^{-a_4 v_m}, \qquad k_{vc} = k_{1c} e^{-a_4 v_m}, \tag{9}$$

$$v_m = \sqrt{(x_r)^2 - \dot{x}_r x_r}. \tag{10}$$

The model requires identification of a total of 16 parameters ($F_0$, $I_0$, $I_1$, $a_0$, $a_1$, $a_2$, $a_3$, $a_4$, $k_0$, $k_{1c}$, $k_{1e}$, $k_2$, $k_3$, $k_4$, $k_5$, $k_6$) from the measured data for the asymmetric characteristics, and can be simplified to characterize the symmetric $f-v$ characteristics by letting $k_5 = k_6 = 0$ and $k_1 = k_{1c} = k_{1e}$. It should be noted that the proposed generalized hysteretic $f-v$ model has a little modification from that in the force offset parameter formulation $F_b$[5].

The generalized hysteretic $f-v$ model synthesis in conjunction with the measured data for the symmetric and asymmetric damping characteristics are used to identify the model parameters. In order to characterize the damping properties over wide ranges of applied current and excitation condition, a cost function $U$ is formulated to incorporate the squared errors corresponding to different test conditions[5-8].

$$U = \sum_{l=1}^{L} \sum_{k=1}^{K} \sum_{j=1}^{J} [F(i_d, v_r)_{j,k,l} - F_d(i_d, v_r)_{j,k,l}]^2. \tag{11}$$

Where $F_{(j,k,l)}$ is the magnitude of measured damping force corresponding to $j^{th}$ coordinate of the hysteron loop, $k^{th}$ current and $l^{th}$ frequency. $F_{d(j,k,l)}$ is the corresponding damping force computed from the model. $J$, $K$ and $L$ define the levels of data points, currents and frequencies considered in the squared sum error function $U$.

Tables 1 and 2 summarize the parameters of the symmetric and asymmetric models identified from the measured data.

**Table 1 Identified symmetric model parameters of the candidate MR-damper**

| Parameter | Asymmetry | Parameter | Asymmetry |
|---|---|---|---|
| $a_0$ | 992.985 | $k_0$ | 125.987 |
| $a_1$, $(m/s)^{-1}$ | 5.197 | $k_1$ | 11.20 |
| $a_2$, $A^{-1}$ | 7.258 | $k_2$ | 9.244 |
| $a_3$, $A^{-1}$ | 6.635 | $k_3$ | 9.186 |
| $a_4$, $(m/s)^{-1}$ | 7.504 | $k_4$ | -0.119 |
| $I_0$, A | 0.079 | $F_0$, N | 68.506 |
| $I_1$, A | 0.267 | | |

**Table 2 Identified asymmetric model parameters of the candidate MR-damper**

| Parameter | Asymmetry | Parameter | Asymmetry |
|---|---|---|---|
| $a_0$ | 995.499 | $k_{1c}$ | 16.877 |
| $a_1$, $(m/s)^{-1}$ | 1.417 | $k_{1e}$ | 4.673 |
| $a_2$, $A^{-1}$ | 5.225 | $k_2$ | 10.61 |
| $a_3$, $A^{-1}$ | 2.441 | $k_3$ | 10.666 |
| $a_4$, $(m/s)^{-1}$ | 2.383 | $k_4$ | -0.125 |
| $I_0$, A | 0.268 | $k_5$ | 0.269 |
| $I_1$, A | 1.131 | $k_6$ | 0.453 |
| $k_0$ | 177.51 | $F_0$, N | 79.92 |

## 3 Model Validations

The proposed generalized hysteretic $f-v$ model is further validated for both symmetric and asymmetric damping properties of the MR-damper by comparing the model results with the measured data, under a wide range of excitation conditions and magnitudes of drive current.

Fig. 5 shows comparisons of the symmetric model results in terms of $f-v$ characteristics with the measured data under different test conditions. Fig. 5(a) illustrates the comparisons under different drive currents ($i_d$ = 0 to 0.4 A) at 1.5 Hz harmonic excitation with amplitude of 12.5 mm. Fig. 5(b) and (c) show comparisons of results under different excitation amplitudes in the 2.5 to 50 mm range, and frequencies in the 0.5 to 5 Hz range, while the applied current is held fixed ($i_d$ = 0.2 A). The above results generally show reasonably good agreements between the symmetric model results and the test data over the entire range of test conditions considered, with the exception of those attained at high frequencies.

The proposed asymmetric hysteretic $f-v$ model is further validated under selected ranges of excitations and drive currents. Fig. 6 illustrates the comparisons of the model results with the measured data under different drive

currents ($i_d$ = 0 to 0.4 A) and low frequency excitations ($f$ = 0.5 and 1.5 Hz, $a_m$ = 12.5 and 25 mm). The comparisons of model results with the measured data generally show reasonably good agreements between the model results and the test data over the range of test conditions considered, irrespective of the applied current and excitation conditions within the lower frequency range.

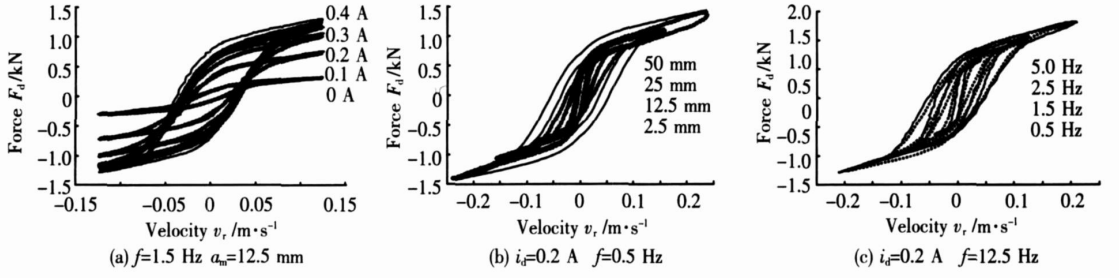


**Fig.5 Comparisons of symmetric model results with the measured data under different excitation conditions**

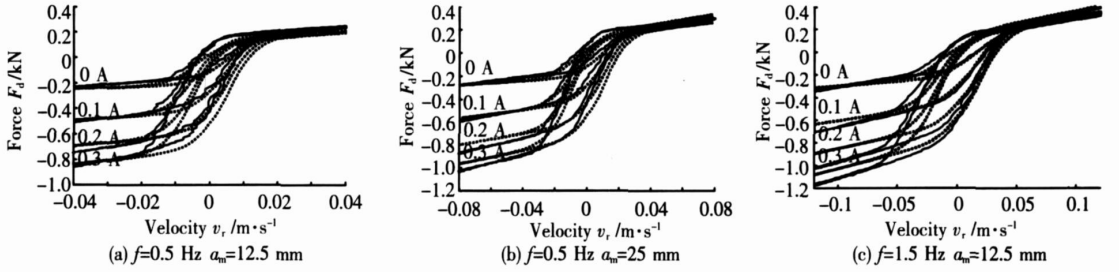


**Fig.6 Comparisons of asymmetric model results with the measured data under low frequency excitations and drive current**

## 4 Conclusion

Extensive laboratory measurements show that the proposed asymmetric damping force generation (ADFG) algorithm is available for generating asymmetric damping force in compression and extension from the symmetric MR-damper, and the proposed generalized model can accurately characterize both symmetric and asymmetric hysteretic $f-v$ characteristics of the MR dampers, irrespective of the excitation conditions and drive currents. The results effectively illustrate that the proposed ADFG algorithm and generalized model could be employed to synthesize advanced semi-active controller for implementation in vehicle suspension with the MR dampers.

**[References]**

[1] Spencer B F, Dyke D J, Sain K M, et al. Phenomenological model of a magneto-rheological damper [J]. J of Eng Mech, 1997, 123(3): 230-238.

[2] Lee H S, Choi S B. Control and response characteristics of a magneto-rheological fluid damper for passenger vehicles [J]. J of Intelligent Material Systems and Structures, 2000, 11(1): 80-87.

[3] McManus S J, St Clair K A E. Evaluation of vibration and shock attenuation performance of a suspension seat with a semi-active magneto-rheological fluid damper[J]. J of Sound and Vibration, 2002, 253(1): 313-327.

[4] Wang E R, Ma X Q, Rakheja S, et al. Modeling hysteretic characteristics of an MR-fluid damper [J]. Procs of the Institution of Mechanical Engineers, J of Automobile Engineering, 2003, 217(D7): 537-550.

[5] Wang E R. Syntheses and analyses of semi-active control algorithms for a magneto-rheological damper for vehicle suspensions [D]. Montreal, Canada: Concordia University, 2005: 41-46.

[6] Wang E R, Ye B M, Chen Y S, et al. Research on generation of asymmetric $f-v$ characteristics from symmetric MR-damper [J]. Chinese J of Mechanical Engineering, 2006, 19(2): 237-242.

[7] Wang E R, Ma X Q, Rakheja S, et al. Generalized asymmetric hysteresis model of controllable magneto-rheological damper for vehicle suspension attenuation [J]. Chinese J of Mechanical Engineering, 2004, 17(2): 301-305.

[8] Wang E R, Wang W J, Wang Hui, et al. Characterization and modelling of symmetric and asymmetric damping properties of a magnetorheological damper [C] // Proc of 7th WSEAS Int Conf on Simulation, Modelling and Optimization (SMO'07), Beijing, 2007: 332-340.

[9] Carrera web site[EB/OL]. http://www.carrerashocks.com, 2002.

[责任编辑: 刘　健]